

This figure "stiavelli.fig1a.jpg" is available in "jpg" format from:

<http://arxiv.org/ps/astro-ph/0012170v1>

This figure "stiavelli.fig1b.jpg" is available in "jpg" format from:

<http://arxiv.org/ps/astro-ph/0012170v1>

This figure "stiavelli.fig1c.jpg" is available in "jpg" format from:

<http://arxiv.org/ps/astro-ph/0012170v1>

Name	mag (F555W)	A_B	distance (Mpc)	M_V	Nucleus?	$(V-I)_{cusp}$ ($0''.1 - 0''.5$)
fcc48	16.55±0.13	0.00	19.1	-14.86	N	0.98±0.03
fcc64	17.09±0.10	0.00	19.1	-14.32	N	1.12±0.10
fcc110	16.49±0.10	0.00	19.1	-14.92	N	1.07±0.05
fcc136	14.32±0.18	0.00	19.1	-17.09	Y	1.15±0.02
fcc150	15.13±0.10	0.00	19.1	-16.28	Y	1.10±0.01
fcc174	16.16±0.10	0.00	19.1	-15.25	Y	1.09±0.01
fcc208	16.69±0.30	0.00	19.1	-14.72	Y†	0.94±0.11
fcc254	16.71±0.21	0.00	19.1	-14.70	Y	0.97±0.07
fcc316	16.17±0.10	0.00	19.1	-15.24	Y	1.27±0.16
fcc324	14.95±0.10	0.00	19.1	-16.46	Y	1.00±0.03
lgc47	14.57±0.10	0.06	11.5	-15.73	N	1.07±0.03
lgc50	16.04±0.21	0.06	11.5	-14.26	Y	1.07±0.09
vcc9	13.21±0.10	0.02	17.4	-17.99	N	1.03±0.02
vcc118	15.55±0.15	0.00	17.4	-15.65	N	0.99±0.03
vcc240	16.34±0.70	0.14	17.4	-14.86	Y	0.98±0.08
vcc452	15.36±0.11	0.01	17.4	-15.84	Y	1.00±0.02
vcc503	16.83±0.10	0.01	17.4	-14.37	Y	0.93±0.07
vcc917	14.76±0.10	0.11	17.4	-16.44	N	1.07±0.01
vcc1073	13.89±0.11	0.07	17.4	-17.31	Y	1.14±0.03
vcc1254	14.82±0.13	0.00	17.4	-16.38	Y	1.05±0.02
vcc1577	15.17±0.31	0.02	17.4	-16.03	N	1.03±0.02
vcc1651	16.08±0.29	0.00	17.4	-15.12	N	1.11±0.11
vcc1762	15.81±0.20	0.00	17.4	-15.39	N	1.01±0.03
vcc1876	14.39±0.18	0.03	17.4	-16.81	Y	1.15±0.05
vcc2029	16.98±0.28	0.02	17.4	-14.22	N	0.92±0.05

Table 1: Apparent, extinction corrected, magnitude in F555W, adopted extinction A_B (Burstein and Heiles 1982), adopted distance in Mpc, absolute magnitude M_V , presence of a nucleus (Miller et al. 1998), and cusp V-I color for the dwarf ellipticals in our sample. † FCC208 was not included in Miller et al. (1998) because its close distance to NGC 1399 makes it hard to determine the globular cluster specific frequency which was the main aim of that paper.

This figure "stiavelli.fig2a.jpg" is available in "jpg" format from:

<http://arxiv.org/ps/astro-ph/0012170v1>

This figure "stiavelli.fig2b.jpg" is available in "jpg" format from:

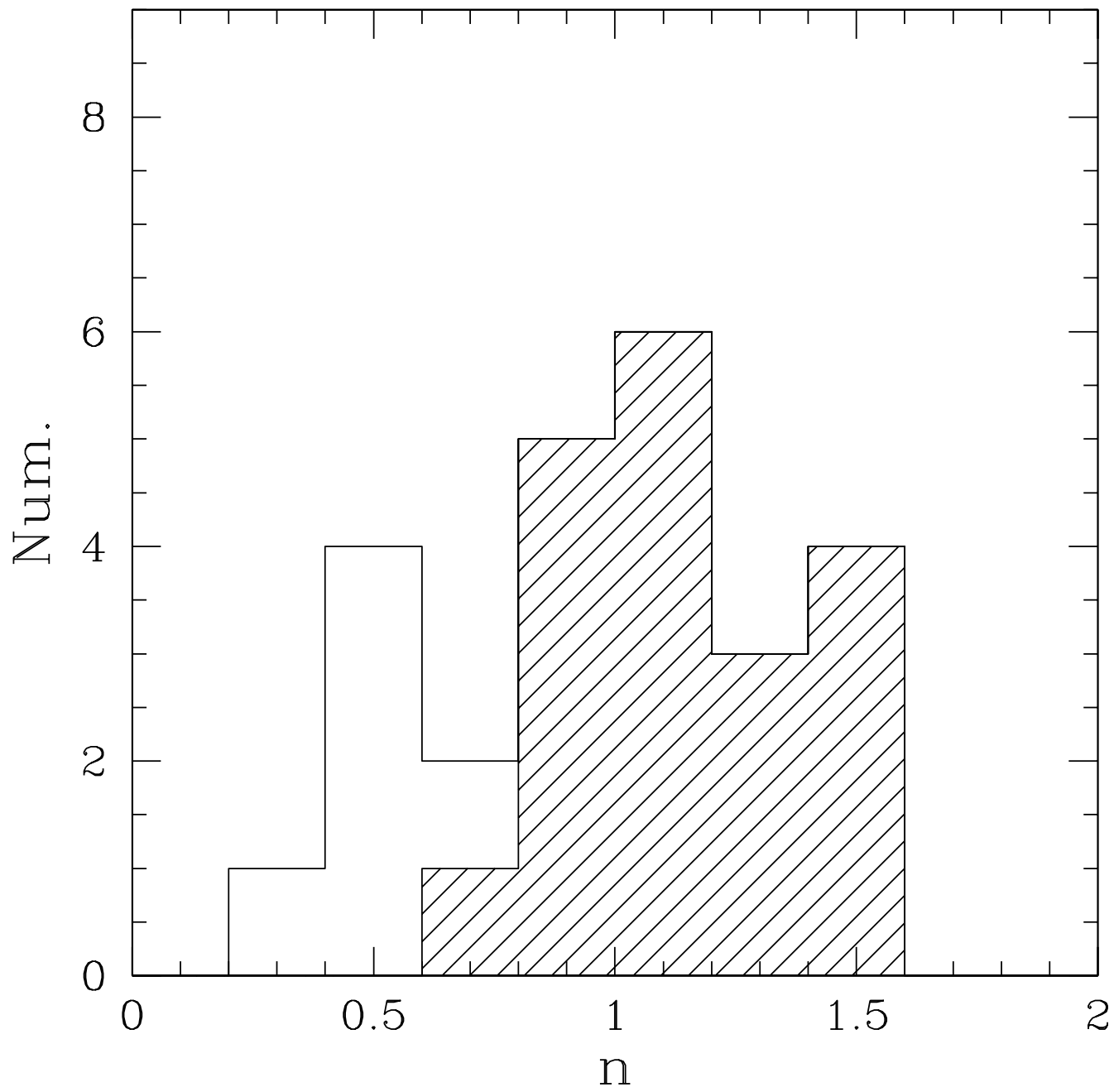
<http://arxiv.org/ps/astro-ph/0012170v1>

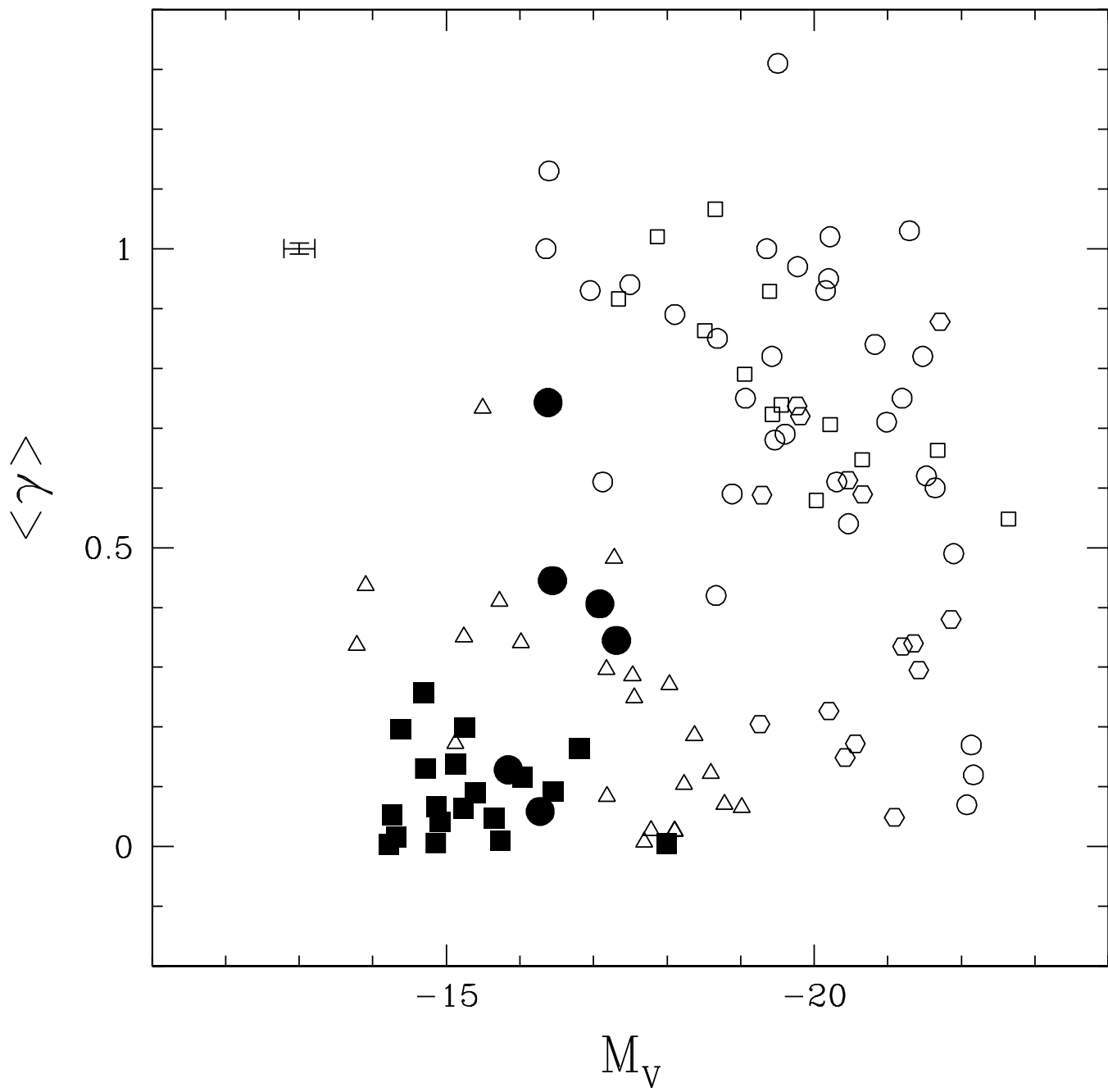
This figure "stiavelli.fig2c.jpg" is available in "jpg" format from:

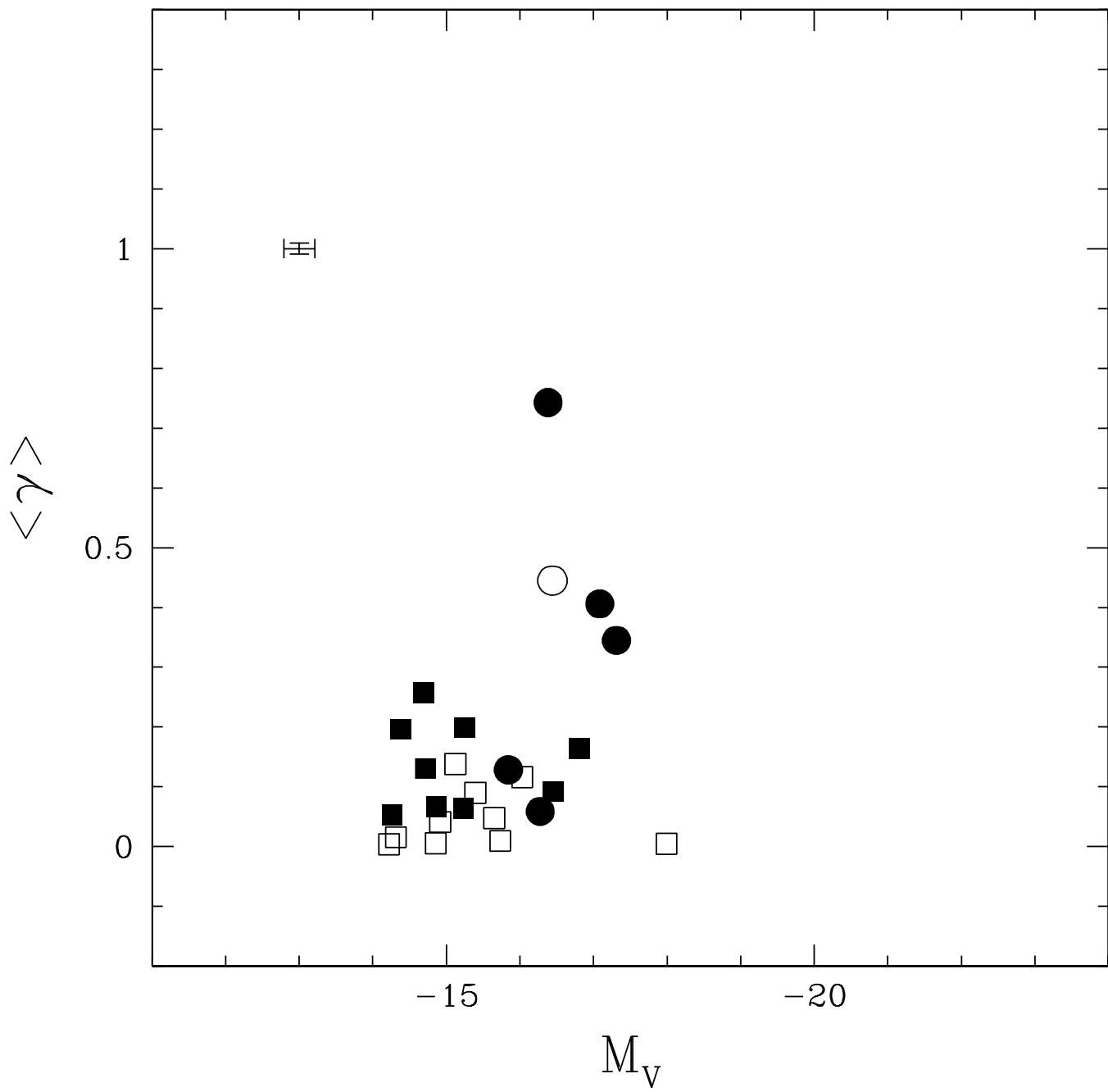
<http://arxiv.org/ps/astro-ph/0012170v1>

Name	r_b (")	α	β	γ	$\langle\gamma\rangle$ (0'1-0'5)	Best Fit (R>1")	Sersic n (R>1")
fcc48	5.28±1.20	2.04±0.29	2.26±0.41	0.0001±0.0001	0.0059±0.0014	expo	0.96±0.07
fcc64	18.88±0.62	1.92±0.08	6.75±0.28	0.0168±0.0010	0.0159±0.0010	expo	1.53±0.20
fcc110	7.42±1.65	2.33±1.13	1.89±0.46	0.0486±0.0257	0.0413±0.0012	expo	1.16±0.07
fcc136	6.37±0.74	1.89±0.25	1.77±0.13	0.4541±0.0234	0.4061±0.0140	seraic	0.49±0.02
fcc150	3.59±0.46	1.37±0.12	2.38±0.17	0.0002±0.0001	0.0589±0.0073	seraic	0.55±0.03
fcc174	5.36±1.23	2.30±0.37	2.68±0.45	0.2295±0.0589	0.1991±0.0065	expo	0.82±0.04
fcc208	8.74±0.29	2.32±0.13	1.89±0.12	0.1536±0.0408	0.1305±0.0060	expo	1.15±0.03
fcc254	46.85±39.2	1.47±0.91	6.54±5.32	0.2949±0.0938	0.2577±0.0110	expo	1.04±0.19
fcc316	28.65±4.92	1.23±0.21	6.42±0.56	0.0551±0.0897	0.0637±0.0036	expo	0.95±0.04
fcc324	9.36±0.68	1.95±0.30	2.12±0.17	0.1074±0.0368	0.0921±0.0045	expo	1.08±0.03
lgc47	10.10±2.63	1.39±0.23	1.64±0.32	0.0001±0.0001	0.0096±0.0022	expo	1.53±0.04
lgc50	7.28±0.96	2.86±0.36	1.66±0.20	0.0632±0.0370	0.0529±0.0091	expo	1.30±0.09
vcc9	7.52±1.91	2.95±0.53	0.97±0.28	0.0055±0.0010	0.0046±0.0007	expo	1.58±0.08
vcc118	10.40±0.79	2.30±0.09	2.71±0.21	0.0566±0.0194	0.0478±0.0035	expo	1.47±0.05
vcc240	22.42±14.4	1.66±0.94	3.06±2.11	0.0779±0.0491	0.0669±0.0034	expo	1.11±0.25
vcc452	4.54±0.51	1.54±0.18	1.78±0.14	0.1302±0.0221	0.1284±0.0053	seraic	0.61±0.03
vcc503	8.88±1.58	3.46±2.62	4.02±1.07	0.2298±0.1028	0.1965±0.0090	expo	1.13±0.19
vcc917	8.54±0.88	1.35±0.09	3.26±0.19	0.5000±0.0141	0.4450±0.0160	seraic	0.45±0.03
vcc1073	4.29±0.26	1.81±0.23	1.63±0.08	0.3843±0.0240	0.3450±0.0130	seraic	0.48±0.01
vcc1254	10.06±0.97	5.32±1.99	1.87±0.22	0.8105±0.0091	0.7426±0.0170	seraic	0.29±0.01
vcc1577	4.58±0.20	3.30±1.37	1.30±0.09	0.1377±0.0370	0.1163±0.0050	expo	0.88±0.05
vcc1651	10.17±1.47	4.29±1.80	1.21±0.26	0.1633±0.0708	0.1383±0.0060	expo	1.85±0.09
vcc1762	6.02±0.74	2.45±0.29	2.28±0.22	0.1055±0.0247	0.0899±0.0040	expo	1.02±0.05
vcc1876	8.08±0.22	2.89±0.27	1.84±0.06	0.1921±0.0126	0.1634±0.0070	expo	1.07±0.03
vcc2029	5.86±0.72	2.11±0.21	2.22±0.23	0.0001±0.0001	0.0039±0.0006	expo	0.97±0.05

Table 2: Nuker fit parameters, average logarithmic slope $\langle\gamma\rangle$, type of light profile, and best fitting Sersic exponent n for the dwarf ellipticals in our sample. See the text for a definition of the parameters.







The nuclear cusp slopes of dwarf elliptical galaxies ¹

Massimo Stiavelli

Space Telescope Science Institute, 3700 San Martin Dr., Baltimore, MD 21218

Bryan W. Miller

Gemini Observatory, Casilla 603, La Serena, Chile

Henry C. Ferguson, Jennifer Mack, and Bradley C. Whitmore

Space Telescope Science Institute, 3700 San Martin Dr., Baltimore, MD 21218

and

Jennifer M. Lotz

Dept. of Physics and Astronomy, Johns Hopkins University, Baltimore, MD, 21218

Received _____; accepted _____

¹Based on observations with the NASA/ESA *Hubble Space Telescope* - GO 6352, obtained at the Space Telescope Science Institute, which is operated by the Association of Universities for Research in Astronomy, Inc., under NASA contract No. NAS5-26555

ABSTRACT

We derive the light profiles for a sample of 25 dwarf elliptical galaxies observed by us with HST/WFPC2 in F555W and F814W. These profiles are fitted with Nuker, $R^{1/4}$, exponential, and Sersic laws, and are also used to derive the nuclear cusp slopes γ . We discuss the correlation of nuclear cusp slope with galactic luminosity, presence of a nucleus, and type of light profile. The results are compared to those found in the literature for elliptical galaxies and the bulges of spiral galaxies. We find that as a class the nuclear regions of dwarf ellipticals are very similar to those of the exponential bulges of spiral galaxies, and have nuclear cusp slopes shallower than those of bulges that were well fitted by a de Vaucouleurs $R^{1/4}$ profile with the same luminosity. For the 14 nucleated galaxies in our sample this conclusion is less certain than for the 11 non-nucleated objects since it relies on an extrapolation of galaxy light under the nucleus. In terms of their light profiles and nuclear properties, most spheroidal stellar systems can be broadly divided into two subclasses: the exponential shallow cusp objects and the $R^{1/4}$, steep cusp objects. Membership of a class does not appear to correlate with the presence of a massive stellar disk.

Subject headings: galaxies: dwarf — galaxies: photometry — galaxies: nuclei

1. Introduction

Dwarf elliptical galaxies are the dominant galaxy population in clusters of galaxies, yet we are still unsure about their formation mechanism and their evolution. In addition, it is not clear whether the nucleated and non-nucleated dwarfs share a common formation and evolution differing only in their typical luminosity, or are separated by more profound differences. In order to better understand the nature of dwarf ellipticals, we have started a systematic study of the properties of nearby dwarf ellipticals (hereafter dE) in the Virgo and Fornax clusters and in the Leo group. We observed 25 dE galaxies with the Wide Field and Planetary Camera 2 (hereafter WFPC2) onboard the Hubble Space Telescope (HST). For each galaxy we obtained a visible F555W and a near-IR F814W image. We have initially focussed our attention on the properties of the globular cluster population in dwarf ellipticals, and our results are presented in Miller et al. (1998). In the present paper we will instead study the nuclear properties of these objects. The extended light profiles will also be derived.

HST observations have deeply affected our view of the properties of the nuclear regions of all types of galaxies. Expanding on early work by Crane et al. (1993), Jaffe et al. (1994) and Lauer et al. (1995) showed that the inner regions of all early-type galaxies regular enough to be studied, present a residual slope in their radial light profiles down to the smallest spatial scales accessible to HST. No galaxy presents a “core” i.e. a flat light profile in the inner regions. Moreover, Lauer et al. (1995) found that the inner cusp slope $\langle\gamma\rangle \equiv -\langle d\text{Log}I(r)/d\text{Log}r\rangle$ is correlated with global galactic properties: bright, boxy ellipticals have the shallowest cusps, i.e., the lowest values of γ , while fainter, diskly ellipticals have the steepest cusps and the highest values of γ .

The sample was later extended to include ellipticals with kinematically decoupled nuclei (KDC, Carollo et al. 1997a,b) and the bulges of spiral galaxies (Carollo & Stiavelli

1998 and references therein). While KDC were found indistinguishable in their nuclear properties from regular ellipticals, the bulges of spirals showed a bimodal behavior: those bulges that were well fitted, outside their nuclei, by a de Vaucouleurs $R^{1/4}$ profile followed and extended to lower luminosities the trend observed for ellipticals, with the fainter systems being characterized by the steepest nuclear slopes. By contrast, the large fraction of bulges well fitted by an exponential light profile outside their nuclei showed a nuclear cusp slope much shallower than that of $R^{1/4}$ bulges with the same luminosity. Since the radial intervals used for determining the nature of the light profile and for measuring the cusp slope were disjoint, Carollo & Stiavelli (1998) argued that this difference was intrinsic and not a mere artifact of exponentials being flatter than $R^{1/4}$ profiles. To prove this they introduced a modified exponential becoming cuspy at small radii and found that no galaxy was well fitted by such a profile and that, in particular, the central star clusters were more compact than what could be obtained with such a cuspy exponential.

If two classes of bulges exist, then a distinct possibility is that dwarf ellipticals are also separated into two classes by their nuclear properties and, perhaps, by their light profiles. The photometric properties of dwarf galaxies have been studied in the past using ground-based data (see, e.g., Binggeli and Cameron 1993, Vader and Chaboyer 1994). These studies revealed the presence of a large variety of light profile shapes in dwarf galaxies but were unable to reveal their nuclear properties since their angular resolution was limited by atmospheric seeing. This paper is devoted to exploring this issue by exploiting high angular resolution HST photometry. In Section 2 we briefly outline the data reduction and describe how the light profiles were derived. A full description of the data reduction is given by Miller et al. (2000). Section 3 addresses the light profile fits to derive cusp slopes and profile type. The correlation of the derived nuclear slopes with other galactic properties are presented and discussed in Section 4.

2. Observations and Data Reduction and Analysis

For a detailed description of the observations and basic reduction we refer to Miller et al. (1998, 2000). Our WFPC2 snapshot images are taken in the F555W (2×230 sec) and F814W (300 sec) bandpasses with the galaxies centered in chip WF3. The two F555W images are combined and cleaned of cosmic rays (hereafter CR) using a program kindly provided to us by Dr. Richard White. The program identifies cosmic ray hits by sigma-clipping. The peak of each cosmic ray is determined using a high threshold (usually 5 sigma) and the extended area around the peak by using a lower threshold (usually 1 sigma). The noise model includes the detector noise, Poisson noise and effects of flat fielding. The clean image is used as a template for identifying cosmic rays in the single F814W image and removing them by interpolation.

Isophotal profiles were derived on the images clean of CR by using the `ellipse` task in the STSDAS/isophote package. This task is based on the software developed by R. I. Jedrzejewski (1987). Isophotes are determined by least square fitting of the ellipse parameters. Departures from purely elliptical isophotes are then computed by a separate minimization once the best ellipses have been determined. The fit was carried out iteratively to mask any area affected by dust. In particular, we first fitted the galaxy without any dust masking and subtracted the resulting model to identify regions where dust was present. Those regions were masked and the fit was repeated again. Since dwarf galaxies are affected very little by dust, and since we had previously tested extensively this procedure by comparison with an independent fitting scheme (Carollo et al. 1997c), we felt that it was not necessary for these objects to carry out isophotal fits on every image using two different algorithms. The isophotal fits were carried out independently on the combined F555W and the F814W images. The profiles in counts were calibrated to magnitudes using the prescriptions by Holtzman et al. (1995), namely, by iterative application of the equations:

$$V = -2.5 \log(DN_{F555W} s^{-1}) + 21.725 - 0.052 \times (V - I) + 0.027 \times (V - I)^2 + 2.5 \times \log 2.006, \quad (1)$$

$$I = -2.5 \log(DN_{F814W} s^{-1}) + 20.839 - 0.062 \times (V - I) + 0.025 \times (V - I)^2 + 2.5 \times \log 2.006 \quad (2)$$

The iterations are started by assuming as initial value of $V - I$ the one derived by the above equations for $V - I = 0$. Three iterations were typically necessary to achieve convergence. Values of surface brightness are derived from the magnitudes by correcting for the pixel area ($0''.1 \times 0''.1$) and for foreground extinction with $A_V = 0.75A_B$ and $A_I = 0.44A_B$. The light and color profiles for the sample galaxies are shown, respectively, in Figures 1 and 2. Note that the observed color profiles in Figure 2 are obtained from direct subtraction of the profiles in magnitudes arcsec^{-2} and as such are not corrected for the different PSF in F555W and F814W nor for the presence of a nucleus or a globular cluster close to the center.

The apparent magnitudes for each galaxy were computed using two different approaches. Firstly, we measured the flux from a $60''$ aperture in the WF3 after sky and bright sources were removed and replaced by a suitable galaxy flux obtained by interpolation. Secondly, we integrated the flux in the best fit to the galaxy surface brightness profile (see Section 3) by extrapolating beyond the last measured point. The two methods have different advantages and disadvantages. The aperture measurement is more sensitive to sky subtraction errors. The method based on the integration of the surface brightness profile is less sensitive to sky subtraction error but suffers from the uncertainties of extrapolating the observed points. We have adopted as apparent magnitude (listed in Table 1) the average of these two measurements and as error the largest between the formal error in the measurements (typically 0.1 mag) and the semi-difference between the two measurements.

In addition to the apparent magnitude, Table 1 lists the adopted extinction, the assumed distance for each of the target galaxies, and their absolute magnitude. The distances given in the table are identical to those used in Miller et al. (1998), and correspond to distance moduli of $(m - M)_0 = 31.2$ for the Virgo cluster, $(m - M)_0 = 30.3$ for the Leo group, and $(m - M)_0 = 31.4$ for the Fornax cluster.

In the following analysis we have adopted the definition of nucleated dE of Miller et al. (1998, see also Table 2) who established the presence of a nucleus simply by inspecting the images. This is possible since dwarf galaxies tend to have especially flat core profiles and rather compact nuclei which, when present, contrast very well with the flat core. Our isophotal fits confirm these identification, i.e., no fainter nucleus has been identified in galaxies considered to be non-nucleated by Miller et al. (1998). Some nuclei are off-center. For this reason, Miller et al. (1998) determined for each galaxy the centering error σ_{proj} and required that a nucleus needed to be within $3\sigma_{proj}$ from the center. Moreover, a nucleus had to have a probability of more than 99 % of not being a globular cluster seen in projection on the nucleus. The off-center nuclear sources in VCC 1577 and VCC 1762 fail the probability and the distance test, respectively, and are therefore considered as globular clusters.

3. Profile fits and cusp slopes

The isophotal profiles have been fitted with a number of analytical profiles following Carollo et al. (1997a,b). The program carries out a fit over a user specified radial interval while taking into account the PSF characteristics of the data. This is done by convolving the model with Tiny Tim (Krist 1999) PSFs obtained for F555W and F814W and a G0 stellar spectrum. We have used both circularized PSFs obtained by deriving the PSF profile and the original PSFs and found the same cusp light profiles and slopes within the errors. Therefore most of the fits have been carried out using the - faster - circularized PSF. Both

the model and the PSF are supersampled by a factor 5 (i.e. each pixel is 0.020 arcsec) in order to avoid artifacts due to steep slopes near the center. The model convolved with the PSF is then resampled and compared to the data. The best-fit profile is thus unaffected by the WFPC2 PSF. We have verified that our results do not depend on the addition of a small (0.005 arcsec) jitter or on changing the stellar spectrum used to generate the PSF to an F or K type; the change in fitted parameters remaining smaller than the error bars.

A general problem faced when fitting light profiles of galaxies with a nucleus is the uncertainty in separating galaxy and nuclear light. For the dwarf galaxies in our sample the nucleus is fainter than the galaxy by 3.7 - 7.4 magnitudes, with 5 magnitudes being a typical value. Its overall contribution to the light is thus negligible even though it dominates at very small radii. We have adopted the approach of restricting our fits to those radii which appear unaffected by the nucleus, i.e., typically outside 0.5 arcsec. Although not nucleated according to the Miller et al. (1998) definition, VCC 1577 and VCC 1762 have a bright source, likely a star cluster, close to their center. We have been able to subtract this source. This was done iteratively by modeling the source as small Gaussian convolved with the PSF and by changing the total source flux and Gaussian width until the nucleus could be subtracted without leaving either light excesses or dips from the otherwise flat core. The results obtained by repeating the fit for these “clean” galaxies agree within the errors with those obtained by radially restricting the fit.

We first fitted the profiles with a “Nuker law” (Lauer et al. 1995, Byun et al. 1996), namely:

$$I(R) = 2^{(\beta-\gamma)/\alpha} I_b \left(\frac{R_b}{R} \right)^\gamma \left[1 + \left(\frac{R}{R_b} \right)^\alpha \right]^{(\gamma-\beta)/\alpha}, \quad (3)$$

where R is the projected radius, and R_b , α , β , γ , I_b are fitted parameters. The cusp slope is derived in two independent ways: either as the γ parameter of the best Nuker fit or as the mean slope between 0''.1 and 0''.5 of the Nuker fit computed as $\langle \gamma \rangle = -\frac{\sqrt{\langle (\log I - \langle \log I \rangle)^2 \rangle}}{\sqrt{\langle (\log R - \langle \log R \rangle)^2 \rangle}}$.

Since our definition of $\langle\gamma\rangle$ relies on the use of the best Nuker fit as an interpolating formula, it is corrected for the WFPC2 PSF and for the possible presence of a central star cluster. For objects without a nuclear star cluster, we checked that the $\langle\gamma\rangle$ slope derived by fitting the whole profile or the radially restricted profile were the same. Generally, as observed also by Byun et al. (1996) and Carollo et al. (1997), there is good agreement between fitted value of γ and the average of the nuclear slope $\langle\gamma\rangle$. For a few objects, namely FCC 48, FCC 150, LGC 47, VCC 2029, the difference between the two estimates is many times larger than the formal errors. However, in these cases the values are close to zero. In Table 2 we list the Nuker fit parameters, including the slope γ , and the derived value of the nuclear cusp slope $\langle\gamma\rangle$. The errors listed are one sigma errors obtained by determining the change in each parameter that increase the χ^2 value of the fit by one. In the following analysis we prefer to adopt the mean slope $\langle\gamma\rangle$ but our results would not be changed by adopting the fitted Nuker parameter γ .

To verify that the shallow values for the cusp slope that we obtain are not purely an artifact of our fitting procedure, we repeated the fit by considering for all galaxies (including those with a central star cluster) the whole radial profile and by using a modified cuspy exponential profile as the fitting function (see also Carollo & Stiavelli 1998). This tests whether the central star clusters are actually cusps within otherwise shallow cores. We find that in no case does the cuspy exponential provide a good fit for meaningful values of the fitted parameters.

Finally, we repeated our fits by using exponential profiles, $R^{1/4}$ profiles, and Sersic (1968) R^n profiles. These fits were typically performed outside 1" radius. The goodness of fit was computed by estimating the value of χ^2 per degree of freedom. The error on the Sersic exponent has been found by requiring the χ^2 value to increase by one. Not surprisingly (see, e.g., Binggeli & Cameron 1991 and Durrell 1997), we find that no galaxy

in our sample is well described by an $R^{1/4}$ law. The closest object to an $R^{1/4}$ profile is VCC 1254 with a Sersic slope $n = 0.29 \pm 0.01$. Out of 25 galaxies, 19 are well fitted by a simple exponential profile, while 6 are described by Sersic profiles with n significantly different from both 0.25 and 1 which are the values giving an $R^{1/4}$ or an exponential, respectively (see Table 2). Generally, for those objects that are fitted equally well by an exponential and a Sersic model, the two fits look very similar. The one exception being FCC208 where a bump in the light profile is fitted by the Sersic law and not by the exponential. Since the nucleus in FCC208 departs from a point source, it is hard to establish whether the feature should be considered part of the nucleus or part of the galaxy. We think that it is likely that the bump arises from a PSF feature and have chosen to consider it as part of the nucleus and adopt the exponential fit. Clearly, adopting the Sersic fit for this object would not have significantly changed our conclusions. If we took the error on the Sersic exponent n at face value, then for 13 out of 25 objects the exponent n is different from one at the three sigma level. However, in some of these cases, the exponent is close to one so that the model profile remains essentially indistinguishable from an exponential. Note that for bulges of spiral galaxies Carollo et al. (1997c) and Carollo & Stiavelli (1998) found that most galaxies regular enough to derive isophotal profiles could be described by either exponentials or $R^{1/4}$ laws. Only a few bulges could not be fitted by either and would presumably be fitted by a Sersic law. The fitted dE profiles are shown in Figure 1 (solid line for the best exponential fit and dashed line for the best Sersic fit) and are used to obtain color profiles unaffected by central sources or PSF dependencies shown in Figure 2. The average color in the $0''.1$ - $0''.5$ region is given in Table 1. In Figure 3 we plot the histogram of the derived Sersic slopes for the sample identifying by shading those objects that are also well fitted by an exponential profile. As expected, the Sersic exponents cluster around unity for those galaxies with light profiles also well fitted by exponential profiles. On the contrary, it is for those objects with Sersic slope $n \simeq 0.5$ that neither an $R^{1/4}$ or an exponential profile provide adequate fits and

thus the extra parameter in the Sersic law is essential to obtain a good fit.

4. Results and Discussion

As other galaxies observed with HST (Crane et al. 1993, Carollo et al. 1997), dwarf galaxies are characterized by very shallow nuclear color gradients. Some residual gradients can be seen in objects containing a compact source near the nucleus but this is probably due to an imperfect subtraction of the nuclear light.

Dwarf elliptical galaxies are generally characterized by shallow nuclear cusp slopes. This conclusion is direct for non-nucleated galaxies but relies on an extrapolation of the light profile below the nucleus for nucleated objects. While the uncertainties in this extrapolation for nucleated galaxies make this conclusion less robust for these objects, the general similarity in derived properties for nucleated and non-nucleated galaxies increases our confidence on this result.

In Figure 4 we show the correlation of the average nuclear cusp slope $\langle\gamma\rangle$ with the absolute magnitude M_V for dEs and other spheroidal stellar systems. In particular we include elliptical and lenticular galaxies (Burstein et al. 1987; Bender et al. 1993) and bulges of spiral galaxies (Carollo & Stiavelli 1998). The dE objects as a class appear to occupy roughly the same region of the $\langle\gamma\rangle$ - M_V plane occupied by exponential bulges of spiral galaxies. The nuclear slopes of dE galaxies are much shallower than those of the low-luminosity end of the bright elliptical sequence. Moreover, the few dEs characterized by steeper cusps are better fitted by Sersic profiles (see also Table 2) rather than exponentials. There is also an indication that dwarfs with a light profile well described by an exponential profile have somewhat shallower nuclear slopes than exponential bulges of the same luminosity.

The location of a galaxy in the $\langle \gamma \rangle$ - M_V plane appears to be mildly influenced by the nucleated/non-nucleated nature of the dE (Figure 5). Indeed, by adopting the definition of nucleated dE of Miller et al. (1998, see also Table 2), we find that nucleated galaxies have systematically steeper slopes than non-nucleated ones. However, a decrease in the cusp slopes of nucleated galaxies by only 0.1 would produce a significant overlap between nucleated and non-nucleated objects. Unfortunately, we cannot exclude with confidence the possibility that the higher cusp slopes measured in nucleated dwarfs might be due to a systematic effect in separating galaxy light from that of the nucleus. If part of the effect is real rather than an artifact of the fitting, this would agree with the indication that exponential bulges of spirals, that are all nucleated, have a somewhat steeper light profiles than non-nucleated dwarf ellipticals. However, one of the steepest cusps is observed in VCC 917 which is non nucleated (but has a Sersic profile).

We have verified that neither the nuclear slope $\langle \gamma \rangle$ nor the profile type (exponential or Sersic) seem to correlate with the specific globular cluster frequency S_N (as given by Miller et al. 1998). Similarly, we do not see any correlation between cusp slope and cusp color.

Our findings demonstrate that the anti-correlation between nuclear slope and spheroid luminosity seen in bright elliptical galaxies breaks down for dwarf ellipticals. With regard to their nuclear properties dwarf ellipticals are more closely related to the exponential bulges of spiral galaxies than to bright elliptical galaxies. This is particularly interesting in light of the possibility that some dwarfs ellipticals may actually be the bulges of stripped spirals (Kormendy 1985). Regardless of the specific formation processes, it appears that spheroidal stellar systems can be broadly subdivided into two classes sharing the same light profile and nuclear properties regardless of the presence of a surrounding stellar disk.

We thank Marcella Carollo and Tim de Zeeuw for discussions and an anonymous referee for comments that helped improve the paper. MS thanks the Lorentz Center of

Leiden University where some of this work was carried out, the European Space Agency for support and the Scuola Normale Superiore of Pisa for hospitality. Support for this work was provided by the STScI DDRF grant D001.82173 and NASA through grant number GO-06532.01-95A from the Space Telescope Science Institute, which is operated by AURA under NASA contract NAS5-26555.

REFERENCES

- Bender, R., Burstein, D., Faber S.M. 1993, ApJ, 411, 153
- Binggeli, B., Cameron, L.M. 1991, AA, 252, 27
- Binggeli, B., Cameron, L.M. 1993, AAS, 98, 297
- Burstein, D., Davies, R.L., Dressler, A., Faber, S.M., Stone, R.P.S., Lynden-Bell, D., Terlevich, R., Wegner, G. 1987, ApJS, 64, 601
- Burstein, D., Heiles, C. 1982, AJ, 87, 1165
- Byun, Y.-I., Grillmair, C.J., Faber, S.M., Ajhar, E.A., Dressler, A., Kormendy, J., Lauer, T.R., Richstone, D., Tremaine, S. 1996, AJ, 111, 1889
- Carollo, C.M., Franx, M., Illingworth, G.D., Forbes, D.A. 1997a, ApJ, 481, 710
- Carollo, C.M., Danziger, I.J., Rich, R.M., Chen, X. 1997b, ApJ, 491, 545
- Carollo, C.M., Stiavelli, M., de Zeeuw, P.T., Mack, J. 1997c, AJ, 114, 2366
- Carollo, C.M., Stiavelli M. 1998, AJ, 115, 2306
- Carollo, C.M., Stiavelli, M., Mack, J. 1998, AJ, 116, 68
- Crane, P., Stiavelli, M., King, I.R., et al. 1993, AJ, 106, 1371
- Durrell, P.R. 1997, AJ, 113, 531
- Holtzman, J. A., et al. 1995, PASP, 107, 1065
- Jaffe, W., Ford, H.C., O’Connell, R.W., van den Bosch, F.C., Ferrarese, L. 1994, AJ, 108, 1567
- Jedrzejewski, R. I. 1987, MNRAS, 226, 747

- Kormendy, J. 1985, ApJ, 295, 73
- Krist, J., Hook, R. 1999, “The Tiny Tim User’s Guide”, STScI 530d512
- Lauer, T.R., Ajhar, E.A., Buin, Y.-I., Dressler, A., Faber, S.M., Grillmair, C., Kormendy, J., Richstone, D., Tremaine, S. 1995, AJ, 110, 2622
- Miller, B.W., Lotz, J.N., Ferguson, H.C., Stiavelli, M., Whitmore, B.C. 1998, ApJ, 508, L133
- Miller, B.W., et al. 2000, in preparation
- Sersic, J.-L. 1968, *Atlas de Galaxias Australes*, Cordoba: Obs. Astron.
- Vader, J.P., Chaboyer, B. 1994, AJ, 108, 1209

Fig. 1.— Light profiles for the sample galaxies. Only about 20 points are shown to avoid clutter. The solid lines are the best exponential fits while the dashed lines are the best Sersic fits to the light profiles. For some galaxies the two curves are essentially identical. The adopted model is indicated in each panel below the galaxy name.

Fig. 2.— Color profiles for the sample galaxies. The observed V-I profiles inside 1'' are affected by compact sources at or near the center which may have different colors from the underlying population. The solid lines are the colors derived from the independent exponential or Sersic fit to the V and I profiles and therefore are corrected for PSF and do not include the effect of any central source. Nuclear color gradients appear to be negligible for all the objects.

Fig. 3.— Histogram of the values of the Sersic parameter n derived from the light profile fits. The shaded histogram gives the values for those galaxies with an acceptable exponential fit. No galaxy in our sample is well fitted by an $R^{1/4}$ profile and 6 out of 25 are well fitted by a Sersic profile with slope intermediate between $n=0.25$ and $n=1$.

Fig. 4.— The correlation between nuclear slope $\langle\gamma\rangle$ and absolute magnitude M_V is shown for the dwarf galaxies in our sample (filled symbols) and other objects from the literature. Dwarf ellipticals with exponential light profiles are plotted as filled squares, those with Sersic profiles as filled circles. Open triangles are the exponential bulges of Carollo et al. (1998), the open circles are the $R^{1/4}$ bulges from Carollo et al. (1998). The squares are elliptical galaxies from Lauer et al. (1995) and the hexagons ellipticals from Carollo et al. (1997). The error bars in the upper left corner represent the median error.

Fig. 5.— We show the effect of the presence of a nucleus on the nuclear slope by plotting nucleated dwarf ellipticals (filled symbols) and non-nucleated dwarfs (open symbols) on the $\langle\gamma\rangle$ - M_V plane. Galaxies with a Sersic profile are represented by circles, those with an

exponential profile by squares. The error bars in the upper left corner represent the median error.